Supporting Information

Unveiling the unique promotion of samarium in polyoxometalate catalyzed selective oxidation of benzyl alcohol

Su-Yuan Feng,[a,b,d] Zhong-Yi Rong,[a,c,d] Qinwei Chen,[a,b,d] Xiao-Yuan Wu,[a] Weiming Wu,[a] Sa-Sa Wang *[a,b] and Can-Zhong Lu *[a,c,d]

[a] State Key Laboratory of Structural Chemistry, CAS Key Laboratory of Design and Assembly of Functional Nanostructures, and Fujian Provincial Key Laboratory of Nanomaterials, Fujian Institute of Research on the Structure of Matter, Chinese Academy of Sciences, Fuzhou, 350002, China

[b] College of Chemistry and Materials Science, Fujian Normal University, Fuzhou 350117, China

[c] School of Physical Science and Technology, Shanghai Tech University, Shanghai, 201210, China

[d] Fujian College, University of Chinese Academy of Science, Fuzhou, 350002, China

Materials and Methods.

All chemicals used in this study were of analytical grade, obtained from commercial sources, and were used without further purification. The single-crystal X-ray diffraction (SCXRD) data of Ce-POM were collected at 150 K on Oxford Diffraction/Agilent SuperNova (dual source) diffractometer using Cu Kα radiation, and those of Sm-POM were collected at 100 K on XtaLAB Synergy R, HyPix using Mo Kα radiation. Calculations were performed with the SHELXL-2018/3 program package, and the structures were solved by a direct method and refined on F^2 by the full-matrix least-squares method. TGA were performed with a TGA/DSC 1 STAR^e system in a temperature range of 30−800 °C at a heating rate of 10 °C/min under N_2 atmosphere. Element analysis was conducted on vario MICRO. FT−IR spectra were collected by a VERTEX 70 infrared analyzer. PXRD was carried out on a Rigaku desktop MiniFlex 600 diffractometer with Cu Kα radiation (λ = 1.54184 Å). SEM and EDS mapping was performed on Apreo 2S HiVac. XPS spectra were obtained on an ESCALAB 250Xi (Thermo Fisher) using Al Kα X-ray sources. The binding energy was referenced to the C 1s peak at 284.8 eV. Data were analyzed with the software Avantage. EPR tests were performed on Bruker E500. The results of the catalytic oxidation reaction were analyzed via a gas chromatograph (GC, Agilent 6820, FID) equipped with an HP-5MS capillary column.

Synthesis of $(C_2H_8N)_4Na_4[Se_2W_{18}O_{62}(H_2O)_2]\cdot 13H_2O$ ($\{Se_2W_{18}\}$)

The preparation of $\{Se_2W_{18}\}$ followed a modified procedure. [1] $Na_2WO_4\cdot 2H_2O$ (10.0 g, 30.3 mmol) and Na_2SeO_3 (0.58 g, 3.37 mmol) were dissolved in 200 mL of water. The pH value of the solution was adjusted to 4.8 by 50% acetic acid solution. After stirring for 30 min, dimethylamine hydrochloride (7.9 g, 96.8 mmol) was added in the solution. The final pH was kept at 3.6 by 6 M HCl. After stirring for another 10 min, the solution was heated to 60 °C and kept for 1 h with stirring. Upon the solution cooled down to room temperature, it was filtered and left to evaporate slowly. Colorless needle-shaped crystals were obtained after 3 days, which were then collected by filtration

and air-dried. Yield: 1.0 g (12% based on W).

Synthesis of $(NH_4)_6Na_{18}[Se_6W_{39}O_{141}(H_2O)_3]\cdot 60H_2O$ ($\{Se_6W_{39}\}$)

Precursor $\{Se_6W_{39}\}$ was prepared according to previous literature. [2] $Na_2WO_4\cdot 2H_2O$ (40.0 g, 121.3 mmol), Na_2SeO_3 (4.0 g, 23.1 mmol) and NH_4NO_3 (1.5 g, 18.7 mmol) were successively dissolved in 400 mL of water with stirring. The pH of the solution was then adjusted to 4.0 by 70% HNO_3 and maintained at this value for 5 minutes. Subsequently, the solution was filtered. The filtrate was collected in a 500 ml beaker and allowed to stand at 4 °C. Large colorless needle-shaped crystals of $\{Se_6W_{39}\}$ were collected after two days. Yield: 7.0 g (19.2 % based on W).

Synthesis of $(C_2H_8N)_4\{[Ce_4(H_2O)_{24}][Se_2W_{18}O_{62}(H_2O)_2]_2\}\cdot 27H_2O$ (Ce-POM)

Precursor $\{Se_6W_{39}\}$ (150 mg, 0.01 mmol) was dissolved in 2 mL of water, and then 2 mL dimethylamine hydrochloride (150 mg, 1.84 mmol) aqueous solution was added to prepare solution A. Solution B was prepared by mixing HNO_3 (0.1 ml, 8 mol L^{-1}) and $Ce(NO_3)_3\cdot 6H_2O$ (65.1mg, 0.15 mmol) in 2 mL of water. Then solution B was dropwise added into solution A. The mixture was constantly stirred for 10 min, and then heated at 80 °C for 1 h. After cooling down to ambient temperature, solids were filtered out and filtrate was left for slow evaporation. Light yellow prism crystals of Ce-POM were obtained after 1 week. Yield: 0.048 g (32.0 % based on W). CCDC number 2521229. Element analysis found (%): C 0.95, H 1.48, N 0.62; calculated for C8H142N4O179Se4Ce4W36 (%): C 0.90, H 1.34, N 0.53. ICP-MS: Ce 5.2%, W 61.6%; calculated for C8H142N4O179Se4Ce4W36: Ce 5.3%, W 62.1%. The numbers of $C_2H_8N^+$ and crystal water were determined by the combination of TGA and element analysis.

Synthesis of $(C_2H_8N)_4\{[Sm_4(H_2O)_{24}][Se_2W_{18}O_{62}(H_2O)_2]_2\}\cdot 27H_2O$ (Sm-POM)

The synthetic procedure for Sm-POM is the same as that for Ce-POM except $SmCl_3\cdot 6H_2O$ (47.4mg, 0.13 mmol) was used instead of $Ce(NO_3)_3\cdot 6H_2O$. Colorless prism crystals of Sm-POM were obtained after 1 week. Yield: 0.074 g (49.0 % based on W).

CCDC number 2521238. Element analysis found (%): C 0.81, H 1.38, N 0.59; calculated for C8H142N4O179Se4Sm4W36 (%): C 0.90, H 1.34, N 0.52. ICP-MS: Sm 5.2%, W 60.5%; calculated for C8H142N4O179Se4Sm4W36: Sm 5.6%, W 61.9%. The numbers of $C_2H_8N^+$ and crystal water were also determined by the combination of TGA and element analysis.

General procedure of catalytic reactions

For a typical reaction, substrate, H_2O_2, catalyst, and solvent were successively added into a 10-mL reaction tube. Then the mixture was warmed for 4 h in a preheated oil bath at target temperature with vigorous stirring. Upon the completion of reaction, the reaction tube was cooled down immediately to room temperature in a water bath. The cooled mixture was added by methylbenzene (internal standard) and 5 mL diethyl ether. After thorough homogenization, the mixture was centrifuged. The supernatant was collected for gas chromatography (GC) analysis. Benzyl alcohol conversion and benzaldehyde selectivity were calculated according to the following equations, respectively.

$$\text{Conversion (\%)} = (1 - f_s \times m_i \times S_s / m_s / S_i) \times 100\%$$

$$\text{Selectivity (\%)} = S_{aldehyde} / (S_{aldehyde} + S_{acid} + S_{ester}) \times 100\%$$

The conversion of alcohol was calculated via internal standard correction method. The symbol f_s represents correction factor of substrate with methylbenzene as the internal standard; m_i represents the mass of internal standard; S_s represents the integral area of substrate on GC; m_s represents the mass of substrate; S_i represents the integral area of internal standard on GC; The selectivity of aldehyde was calculated via area normalization method. $S_{aldehyde}$, S_{acid}, and S_{ester} represent the integral areas of product aldehyde, acid, and ester, respectively.

Table S1 Crystallographic data and structure refinement results of Ce-POM and Sm-POM.

	Ce-POM	**Sm-POM**
Empirical formula	$C_8N_4O_{179}H_{142}Se_4Ce_4W_{36}$	$C_8N_4O_{179}H_{142}Se_4Sm_4W_{36}$
Formula weight	10653.67	10694.65
Crystal system	monoclinic	monoclinic
Space group	$P2_1/n$	$P2_1/n$
a (Å)	15.4720(3)	15.4401(3)
b (Å)	18.5957(3)	18.4946(3)
c (Å)	29.9311(5)	29.7144(7)
α (°)	90	90
β (°)	101.1195(18)	101.201(2)
γ (°)	90	90
Volume ($Å^3$)	8449.9(3)	8323.6(3)
Z	2	2
ρ_{calc} (g cm^{-3})	4.031	4.055
M(mm^{-1})	54.003	27.122
F(000)	8916.0	8802.0
Crystal size (mm^3)	0.22 × 0.08 × 0.03	0.20 × 0.07 × 0.04
θ (°)	2.813 to 75.165	1.773 to 27.103
Index ranges	-19 ≤ h ≤ 16, -22 ≤ k ≤ 23, -37 ≤ l ≤ 37	-19 ≤ h ≤ 19, -23 ≤ k ≤ 21, -36 ≤ l ≤ 37
Final R indexes [I>2σ (I)]	R_1 = 0.0631, wR_2 = 0.1687	R_1 = 0.0536, wR_2 = 0.1303
Final R indexes [all data]	R_1 = 0.0716, wR_2 = 0.1779	R_1 = 0.0714, wR_2 = 0.1422

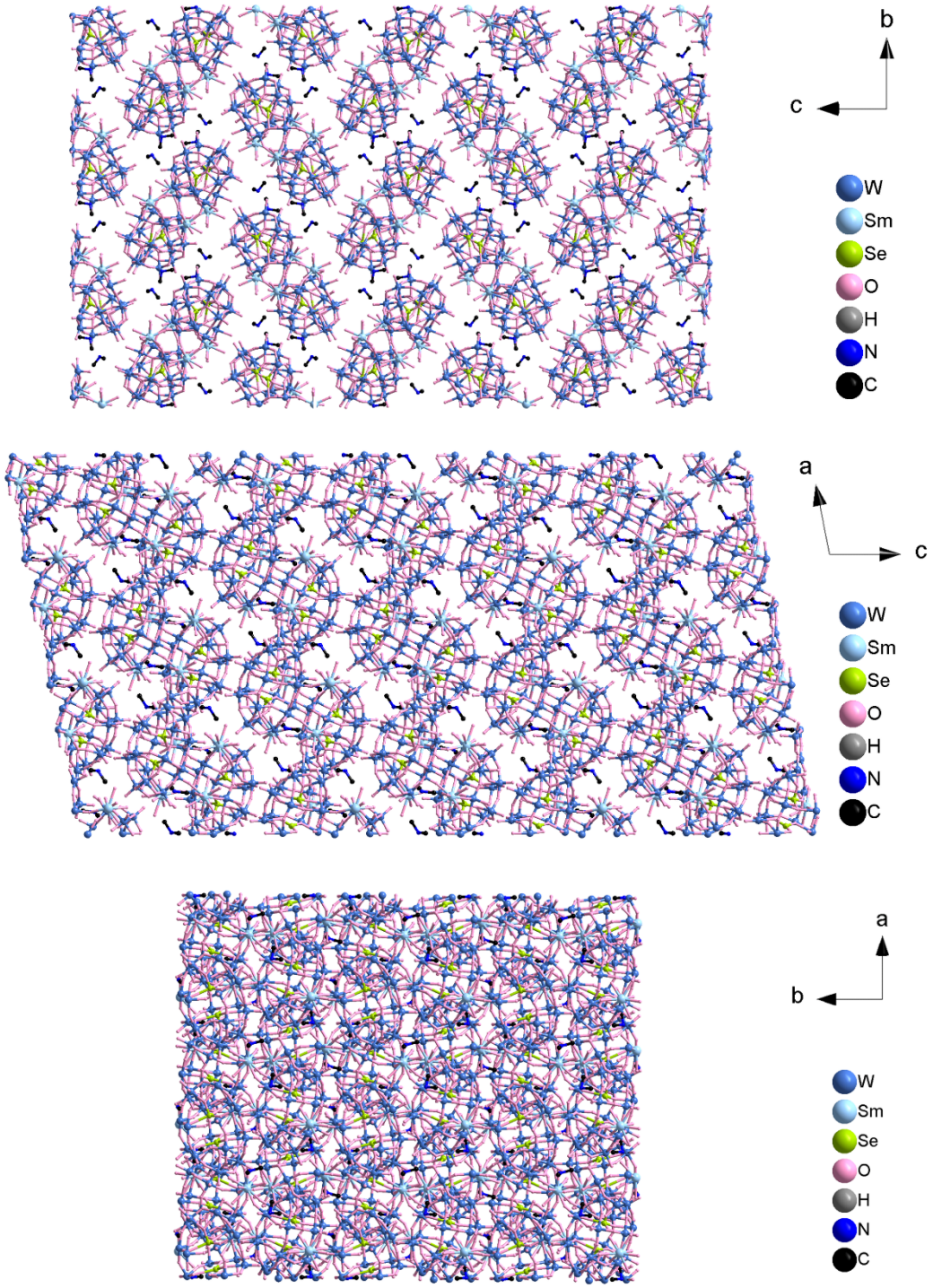

Fig. S1 The packing patterns of Sm-POM viewing from a, b, and c axis.

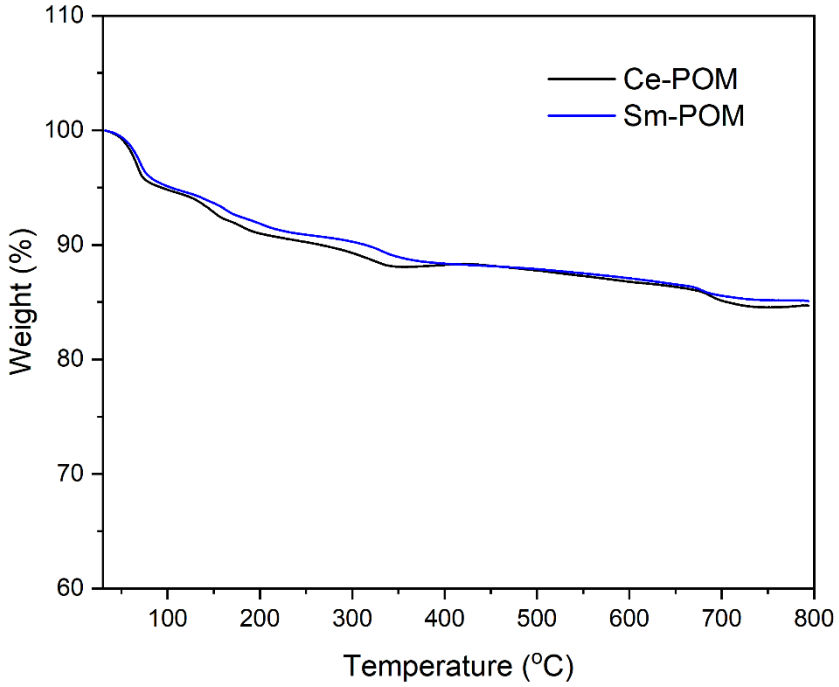

Fig. S2 TGA curves of Ce-POM and Sm-POM under N_2 atmosphere.

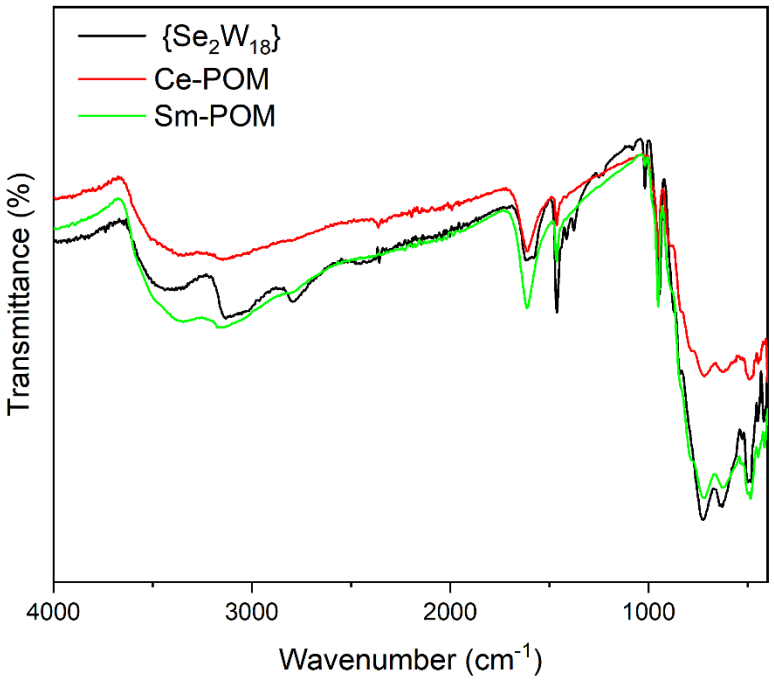

Fig. S3 FT-IR spectra of $\{Se_2W_{18}\}$, Ce-POM and Sm-POM.

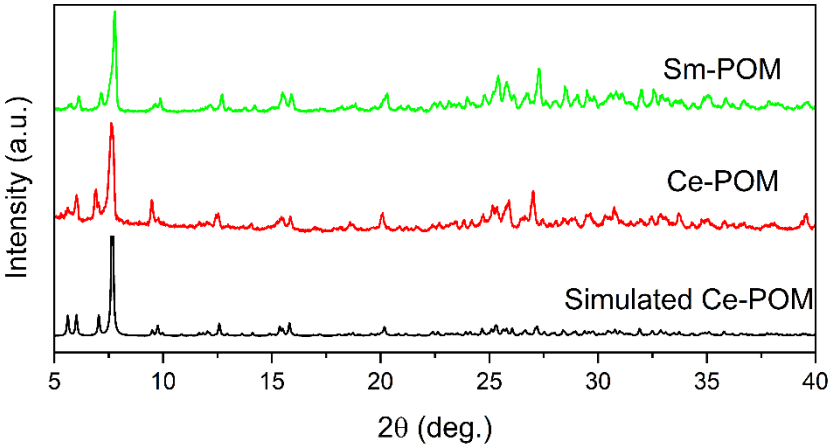

Fig. S4 PXRD spectra of Ce-POM and Sm-POM.

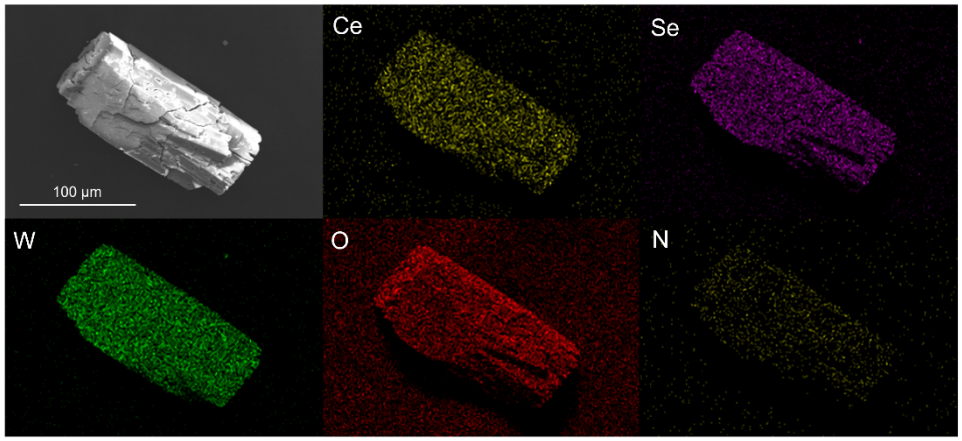

Fig. S5 SEM image and EDS mapping of Ce-POM.

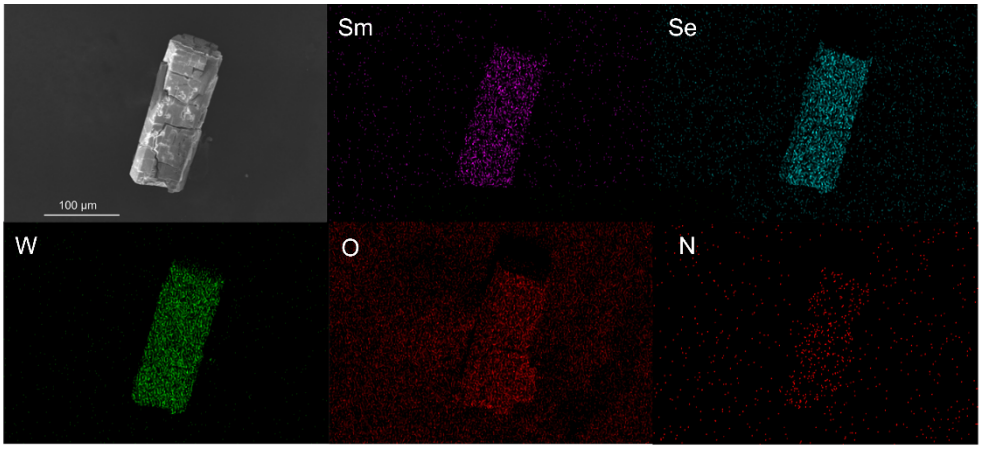

Fig. S6 SEM image and EDS mapping of Sm-POM.

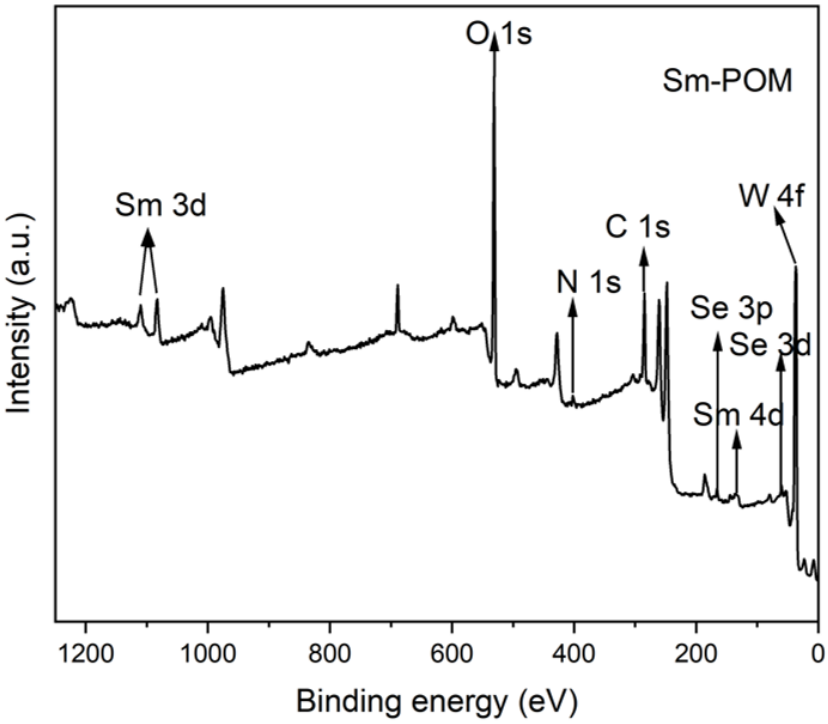

Fig. S7 Survey XPS spectrum of Sm-POM.

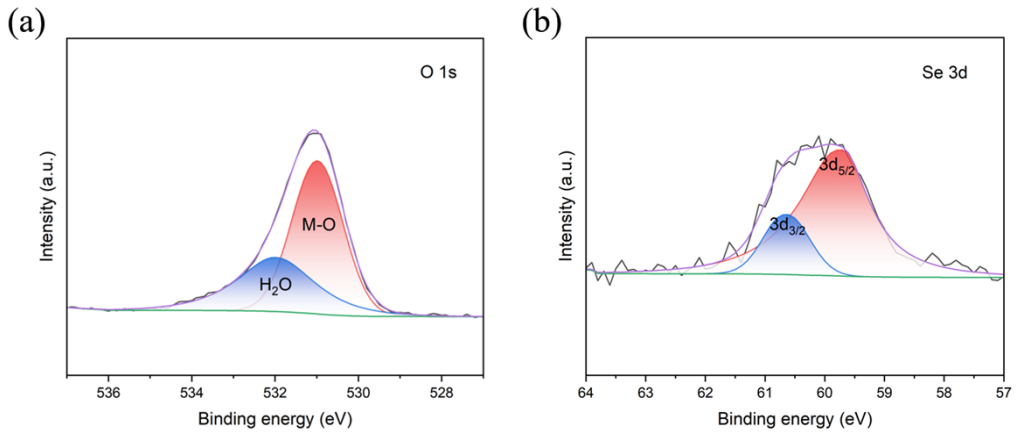

Fig. S8 High-resolution XPS spectra of O 1s and Se 3d in Sm-POM.

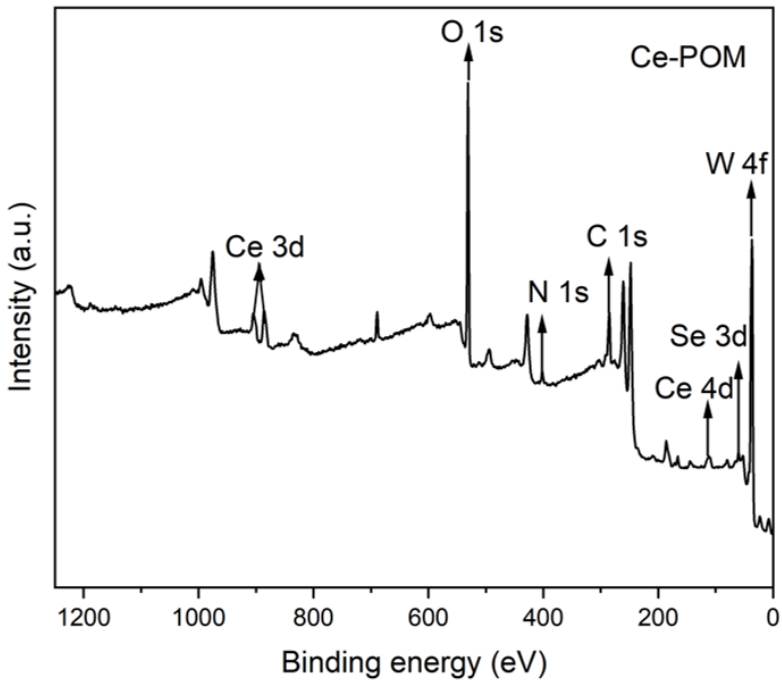

Fig. S9 Survey XPS spectrum of Ce-POM.

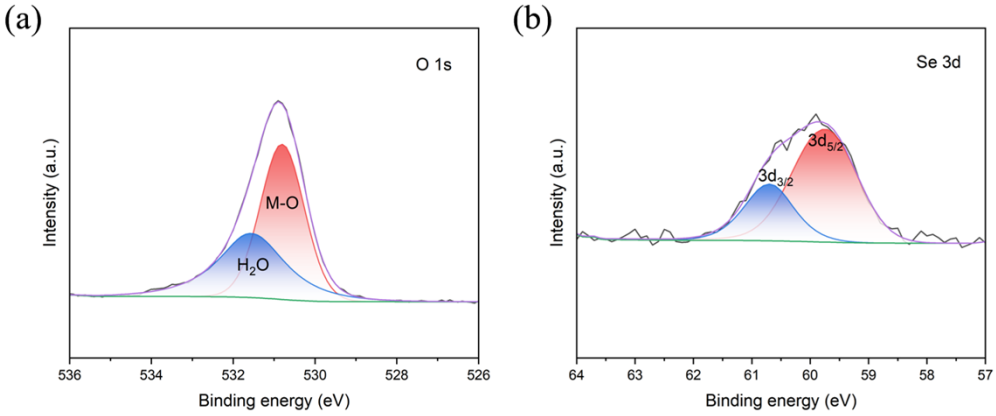

Fig. S10 High-resolution XPS spectra of O 1s and Se 3d in Ce-POM.

Table S2 Activity comparison of Sm-POM with other POM-based catalysts for the catalytic oxidation of benzyl alcohol.

Catalysts	Time (h)	T (℃)	Conversion (%)	Ref.
$[H_2N(CH_3)_2]_{10}H_2[(As_2W_{19}O_{67}(H_2O)(SbO)_2]\cdot 13H_2O$	12.5	60	99.6	[3]
$[H_2N(CH_3)_2]_{14}H_4\{[(As_2W_{19}O_{67}(H_2O)(SbO)_2][P_2W_{18}O_{62}]\cdot 12H_2O$	12.5	60	94.3	[3]
$PMoV_2$@UiO-66-NH_2	4	90	95	[4]
CN-PTA	1	70	70	[5]
PTA@MMS	15	90	97.04	[6]
PTA	15	90	95.5	[6]
$C_{16}H_{64}Cu_4Mo_{10}N_{17}O_{47}V_7$	8	90	96.8	[7]
Sm-POM	4	80	95.11	This work

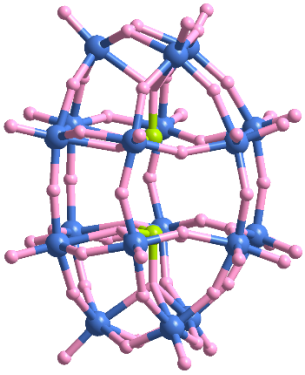

Fig. S11 Structure of $\{Se_2W_{18}\}$.

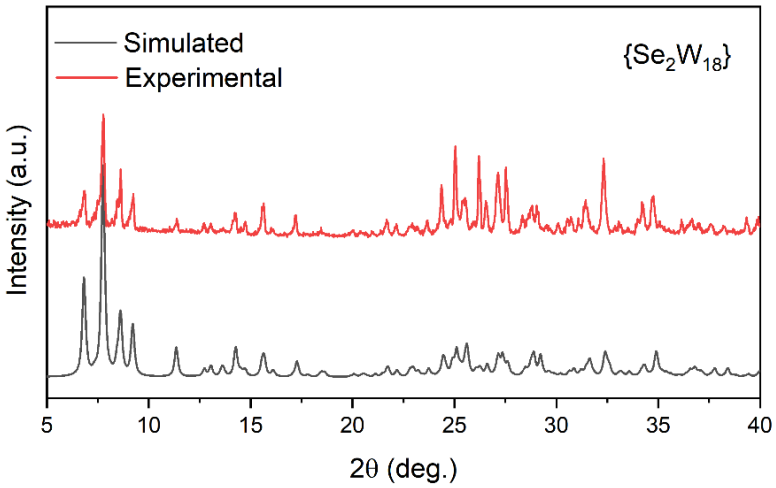

Fig. S12 Simulated and experimental PXRD spectra of $\{Se_2W_{18}\}$.

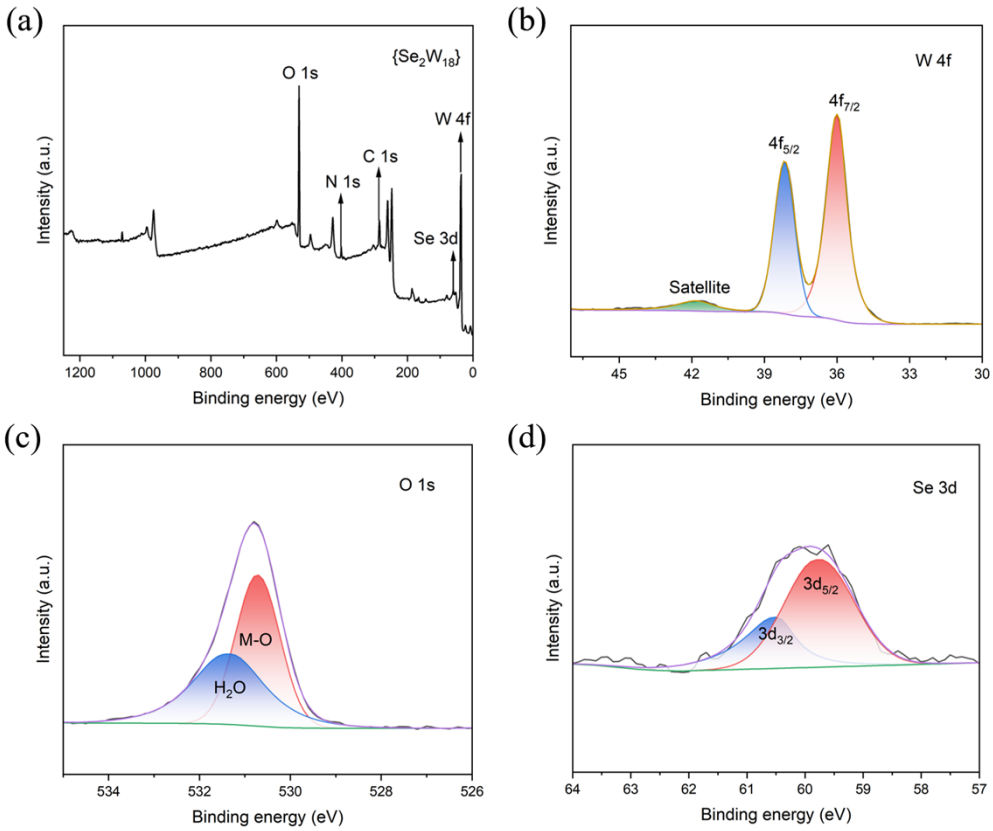

Fig. S13 Survey XPS spectrum of $\{Se_2W_{18}\}$ and high-resolution spectra of W 4f, O 1s, and Se 3d in it.

Table S3 RE···W distance in the structures of RE-POM.

Ce···W distance (Å)		**Sm···W distance (Å)**	
Ce1···W4	4.1537(11)	Sm19···W2	4.1037(11)
Ce1···W6	4.1759(12)	Sm19···W3	4.1052(9)
Ce1···W8	4.0228(12)	Sm19···W4	3.9625(10)
Ce2···W1	4.1508(12)	Sm20···W1	4.0974(10)
Ce2···W4	4.2287(11)	Sm20···W2	4.1650(9)
Ce2···W6	4.1731(11)	Sm20···W3	4.1204(11)
Average Ce···W	4.1508	Average Sm···W	4.0924

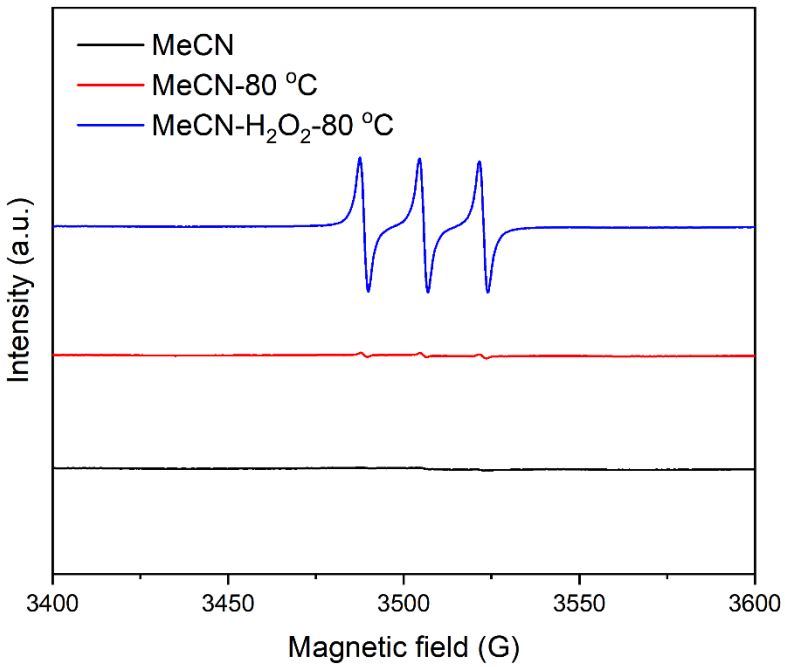

Fig. S14 TEMP-$^1O_2$ signals in MeCN at room temperature, MeCN heated at 80 °C for 4 h, and the mixture of MeCN and H_2O_2 heated at 80 °C for 4 h.

Table S4 Amount of residual H_2O_2 at different times in Sm-POM and Ce-POM mediated systems under optimized condition without benzyl alcohol.

Time	Sm-POM (%)	Ce-POM (%)
0 h	100	100
1 h	86.4	11.3
2 h	46.3	6.5
3 h	33.9	3.1
4 h	32.3	0.7

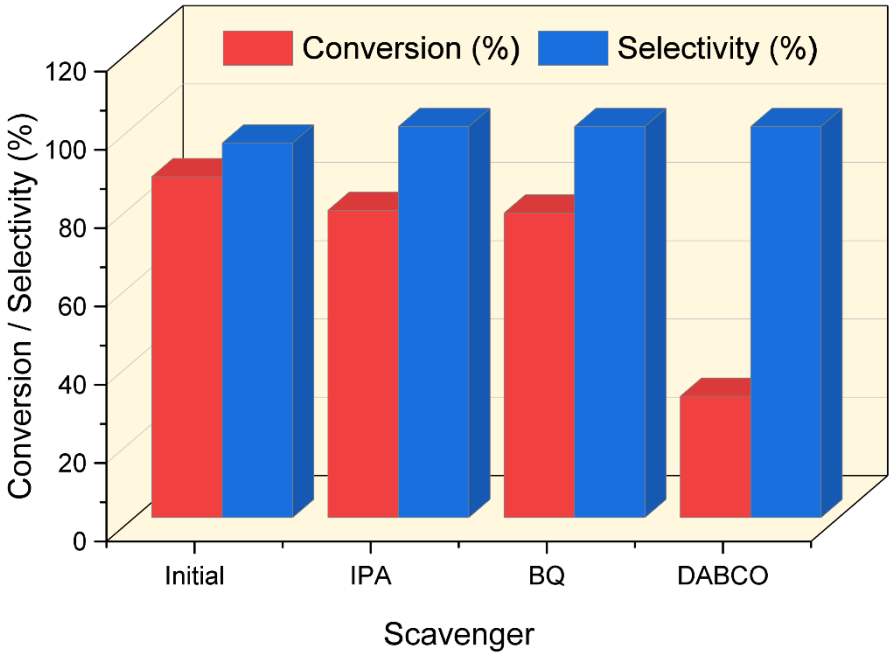

Fig. S15 Scavenging experiments for $\{Se_2W_{18}\}$ catalyzed system (condition: benzyl alcohol 0.25 mmol, $\{Se_2W_{18}\}$ 3.0 μmol, scavenger 0.1 mmol, 30% H_2O_2 1.2 mmol, acetonitrile 1mL, 80 °C, 4 h).

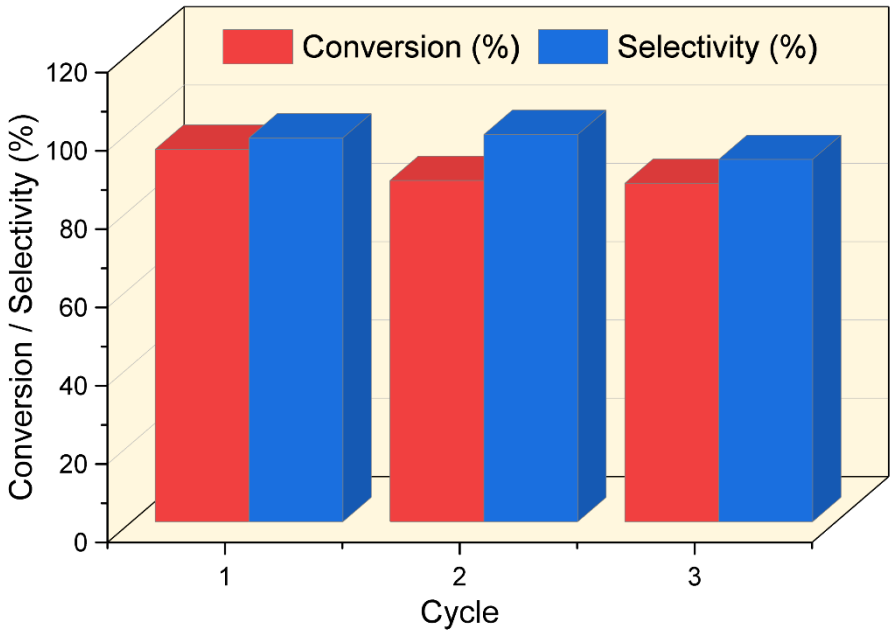

Fig. S16 Recycling catalytic reactions over Sm-POM without catalyst supplement.

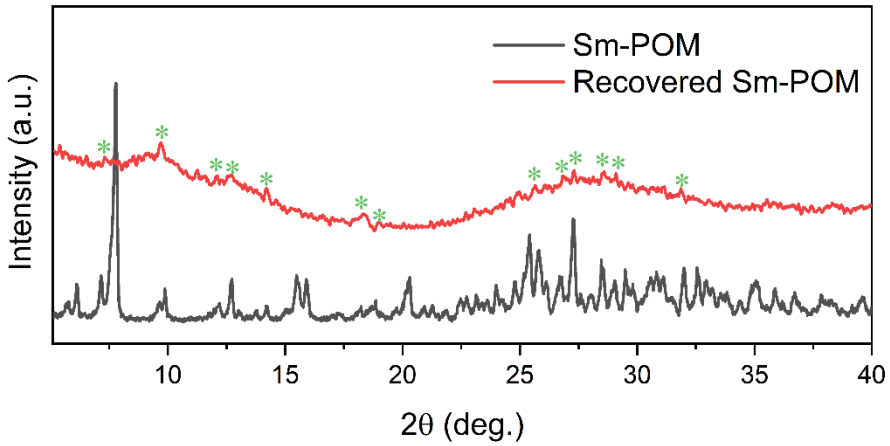

Fig. S17 Comparison of PXRD patterns between fresh Sm-POM and the recovered sample after the 3rd run.

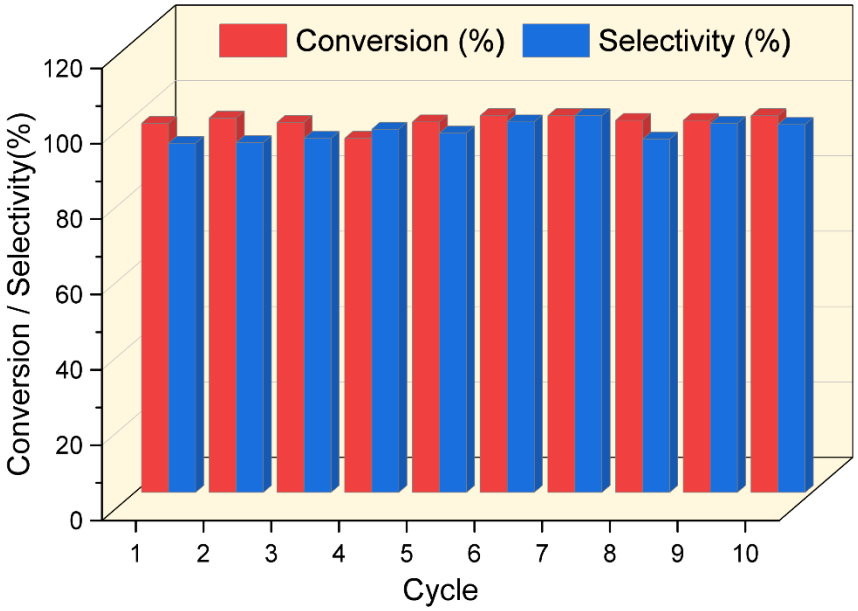

Fig. S18 Recycling catalytic reactions over Sm-POM with catalyst supplement.

Reference

1 W.-C. Chen, L.-K. Yan, C.-X. Wu, X.-L. Wang, K.-Z. Shao, Z.-M. Su and E.-B. Wang, Assembly of Keggin-/Dawson-type Polyoxotungstate Clusters with Different Metal Units and SeO_3^{2-} Heteroanion Templates, *Cryst. Growth Des.*, 2014, **14**, 5099−5110.

2 J. M. Cameron, J. Gao, L. Vilà-Nadal, D.-L. Long and L. Cronin, Formation, Self-Assembly and Transformation of a Transient Selenotungstate Building Block into Clusters, Chains and Macrocycles, *Chem. Commun.*, 2014, **50**, 2155−2157.

3 M. Zhang, L. Liu, Y. Song, M. Hou, P. Ma, Q. Han, Designing Sb - bridged Polyoxotungstates for Efficiently Catalytic Oxidation of Benzyl Alcohol, *J. Catal.*, 2025, **443**, 115957.

4 K. M. Ahmed, K. Amani, A Novel Amine-functionalized Polyoxometalate-based Metal-organic Framework: A Reusable Heterogeneous Nanocomposite for Selective Oxidation of Alcohol, *J. Mol. Struct.*, 2024, **1303**, 137503.

5 H. Li, L. Zheng, Q. Lu, Z. Li, X. Wang, A Monolayer Crystalline Covalent Network of Polyoxometalate Clusters, *Sci. Adv.*, 2023, **9**, eadi6595.

6 R. Chilivery, V. Chaitanya, J. Nayak, S. Seth, R. K. Rana, Heterogenization of Phosphotungstate Clusters into Magnetic Microspheres: Catalyst for Selective Oxidation of Alcohol in Water, *ACS Sustain. Chem. Eng.*, 2022, **10**, 6925–6933.

7 Y. Feng, Z. Zhong, S. Chen, K. Liu, Z. Meng, Improved Catalytic Performance toward Selective Oxidation of Benzyl Alcohols Originated from New Open-framework Copper Molybdovanadate with a Unique V/Mo Ratio, *Chem. Eur. J.*, 2023, **29**, e202302051.